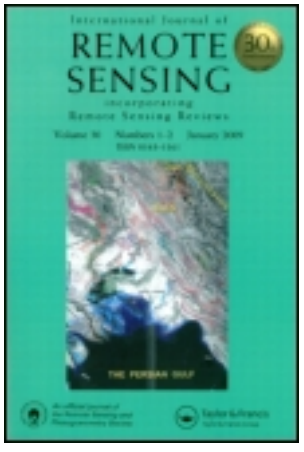

International Journal of Remote Sensing

Publication details, including instructions for authors and subscription information:
http://www.tandfonline.com/loi/tres20

Biomass estimation of mixed forest landscape using a Fourier transform texture-based approach on very-high-resolution optical satellite imagery

Minerva Singh[ac], Yadvinder Malhi[b] & Shonil Bhagwat[cd]

[a] Forest Ecology and Conservation Group, Department of Plant Sciences, University of Cambridge, Cambridge, UK

[b] Environmental Change Institute, University of Oxford, Oxford, UK

[c] School of Geography and the Environment, University of Oxford, Oxford, UK

[d] Faculty of Social Sciences, Open University, Milton Keynes, UK

Published online: 17 Apr 2014.

To cite this article: Minerva Singh, Yadvinder Malhi & Shonil Bhagwat (2014) Biomass estimation of mixed forest landscape using a Fourier transform texture-based approach on very-high-resolution optical satellite imagery, International Journal of Remote Sensing, 35:9, 3331-3349, DOI: 10.1080/01431161.2014.903441

To link to this article: http://dx.doi.org/10.1080/01431161.2014.903441

International Journal of Remote Sensing, 2014
Vol. 35, No. 9, 3331–3349, http://dx.doi.org/10.1080/01431161.2014.903441

Biomass estimation of mixed forest landscape using a Fourier transform texture-based approach on very-high-resolution optical satellite imagery

Minerva Singh[a,c]*, Yadvinder Malhi[b], and Shonil Bhagwat[c,d]

[a]*Forest Ecology and Conservation Group, Department of Plant Sciences, University of Cambridge, Cambridge, UK;* [b]*Environmental Change Institute, University of Oxford, Oxford, UK;* [c]*School of Geography and the Environment, University of Oxford, Oxford, UK;* [d]*Faculty of Social Sciences, Open University, Milton Keynes, UK*

(*Received 16 August 2013; accepted 17 February 2014*)

Assessment of forest structure parameters via remote-sensing data offers the opportunity to examine stand parameters and to detect degradation and forest dynamics, such as above-ground biomass (AGB), at the landscape scale. While much attention has focused on spectrum-based and radar backscatter approaches for assessing forest biomass, texture-based approaches show strong promise. This work makes use of the novel Fourier transform textural ordination (FOTO) method, which involves the combination of 2D fast Fourier transform (FFT) and ordination through principal component analysis (PCA) for characterizing the structural and textural properties of vegetation. This technique presents the potential of Fourier transform approaches in estimating the different forest types, their stand structure, and biomass dynamics in the context of an oil palm–tropical forest landscape in Sabah, Malaysian Borneo. The method was applied to the recordings of very-high-resolution (VHR) Satellite Pour l'Observation de la Terre (SPOT) imagery of the study area. The technique proved useful in distinguishing between the forest types and developing individual biomass estimate models for various forest types. Results show that the FOTO method is able correctly to resolve high AGB values of various forest types. These findings are in agreement with the results based on ground measurements.

1. Introduction

Forest biomass indicates the entire volume of leaf, branch, and stem of all trees and shrubs within the forest ecosystem. Assessing forest biomass, especially the above-ground biomass (AGB) of forests (in dry weight per unit area), is a useful way of quantifying carbon stocks that are being stored/sequestered by a given forest type. Study of forest AGB is also extremely relevant for studying other global biogeochemical cycles and examining how forests respond to the changing climate and extreme events such as drought (Malhi et al. 2009). However, the biomass of each forest component varies by forest type, such as natural or planted forests and closed or open forests (Brown 1997). This makes ecological and field studies in tropical forests difficult because the presence of large, inaccessible regions makes it nearly impossible to perform ground surveys (Gibbs et al. 2007; Pearson et al. 2005), and certain attributes of forest stand parameters, such as the crowns of large canopy trees, are hard to sample (Barker and Pinard 2001; Chambers et al. 2007). Moreover, biomass prediction remains challenging, especially in dense and

*Corresponding author. Email: ms2127@cam.ac.uk

heterogeneous tropical forests (Huete et al. 2002). Satellite remote sensing is an appropriate tool for vegetation mapping and monitoring, as this method provides vital information pertaining to land-use change dynamics at different spatial and temporal scales (Brioch et al. 2011). Recent advances in remote sensing help overcome the above-mentioned obstacles and enable landscape-scale evaluation of forest parameters and dynamics (Ingram, Dawson, and Whittaker 2005; Hawes et al. 2012; Helmer et al. 2012).

AGB estimates derived from satellite imagery involve using vegetation indices, spectral mixture analyses (Souza, Roberts, and Monteiro 2005; Basuki et al. 2012), and radar (Morel et al. 2011), but these techniques are hampered by saturation at high AGB values (Nichol and Sarker 2011; Lu 2006; Woodhouse et al. 2012; Morel 2010). AGB saturation occurs when values are highly concentrated over a small range, making it hard to resolve values beyond a given point or the saturation point.

Over recent years, texture-based approaches have been used to generate estimates of AGB in tropical ecosystems (Wijaya et al. 2010; Lu et al. 2004, 2012; Eckert 2012). Texture has been used as a generic term to describe image properties such as smoothness, regularity, and tonal variation (Jong and van der Meer 2004). Describing the texture of forests, satellite images yield significant information on their structures, thus aiding the accurate estimation of AGB values in areas with complex forest stand structure. Textural ordination is one of the spectral approaches that characterize digital images along coarseness–fineness texture gradients (Barbier, Gastellu-Etchegorry, and Proisy 2010). Fourier transform textural ordination (FOTO) uses a combination of two techniques, namely 2D fast Fourier transform (FFT) for converting spatial information into the frequency domain and ordination by principal component analysis (PCA) (Proisy, Couteron, and Fromard 2007). This method can help classify canopy images with respect to canopy grain and can be used to distinguish between pristine forests and forests with varying logging intensities. This method is further applied to predict biomass from forest canopy parameters that are obtained from remote-sensing data (Couteron, Barbier, and Gautier 2006; Ploton et al. 2012). The basic premise of the FOTO method is that frequency signatures relate well to components of the canopy grain size.

Fourier transforms aid the analysis of the repetitive structure of the canopy by breaking the intensity signal into sinusoidal waves of different spatial frequencies, and have been used as an effective way to analyse specific vegetation data from a wide range of frequencies obtained from very-high-resolution (VHR) satellite data (Barbier, Gastellu-Etchegorry, and Proisy 2010). Satellite Pour l'Observation de la Terre (SPOT) data are then viewed using the ordination method to analyse spatial frequencies within the images in order to quantify the biomass patterns and intensities and estimate AGB (Barbier et al. 2010; Couteron, Barbier, and Gautier 2006). This is an efficient method for analysing specific patterns in the forest biomass, including canopies and related textual vegetation in tropical forest stands (Ploton et al. 2012).

The first major research involving the use of FOTO methods for tropical forests was published by Couteron et al. (2005). FOTO has also been used to estimate forest structural parameters and stand parameters of forests in French Guiana (Proisy, Couteron, and Fromard 2007; Proisy et al. 2012). The FOTO-based model demonstrated better explanatory power on several stand parameters, including basal area, and was not limited by saturation when inspecting dense tropical forests (Ploton et al. 2012). Proisy, Couteron, and Fromard (2007) used FOTO-derived texture indices to generate a biomass model for the mangroves of French Guiana. Ploton et al. (2012) applied the same methodology to generate a FOTO texture indices-based biomass estimate for the Westerns Ghats, India. In both cases, the FOTO-generated AGB displayed a strong correlation with the field AGB

measures, indicating that FOTO is a particularly useful tool for generating remote-sensing-based biomass maps of tropical ecosystems.

This study will deal with a textural approach to estimating biomass with the following objectives: (1) to distinguish between different land-cover types, including forests of different logging intensities, oil palm (OP) plantations, and pristine forests using the FOTO method; (2) to develop texture-based biomass estimate models for the different land-use types; and (3) to determine whether a fragmented forest ecosystem (in this case riparian forests) could be distinguished from surrounding contiguous forest types. The working hypothesis of the paper is that as forest types undergo different levels of disturbance, ranging from light logging to conversion to OP plantations, the canopy structure alters due to the changes in the relative dominance of large-diameter trees and increased dominance of small successional species (in the case of heavily logged forests) or oil palm trees (in the case of oil palm monocultures). For instance, a visual inspection of the aerial photos of old-growth (OG) pristine forests, heavily logged forests, and oil palm plantations in Figure 1 shows that the canopies of these three different forest types are significantly different from each other in terms of their structure and texture.

Thus, we hypothesize that this change can be detected upon examination of the textural properties of the forest canopy. In terms of the technique, FOTO has been implemented according to a detailed methodological description provided by previous authors such as Couteron, Barbier, and Gautier (2006). While no additional technical development has been undertaken in terms of the methodology and algorithms, this research has sought to expand the scope of FOTO for examining an oil palm-dominated mixed forest landscape which also contains fragmented forest zones.

To our knowledge, this paper demonstrates the first use of 2.5m SPOT data (which have a relatively higher resolution compared with the VHR data used in the previous FOTO studies) to distinguish the structure and biomass of forests that have undergone varying logging rotations, oil palm (OP) monocultures, and fragmented tropical forest ecosystem (in this case riparian forests), from the surrounding contiguous forests. In this sense the research also seeks to extend the usage of FOTO to slightly coarser datasets for studying tropical forest ecosystems; something which has not been undertaken by previous studies.

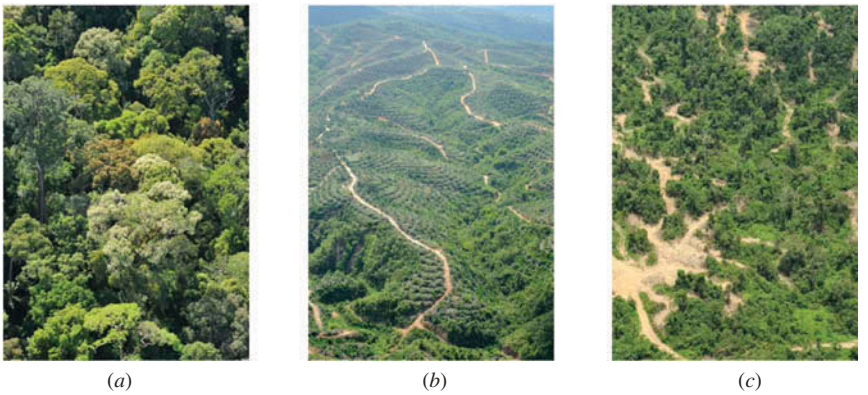

(*a*) (*b*) (*c*)

Figure 1. Aerial view (not scaled) of (*a*) old-growth forests, (*b*) oil palm plantations, and (*c*) experimental area forests (ChienC. Lee, SAFE Project 2011).

2. Materials and methods

2.1. Study area and ground control data

This research was undertaken with the Stability of Altered Forest Ecosystems (SAFE) Project (SAFE Project 2011; Ewers et al. 2011) in Sabah, Malaysia. Figure 2(*a*) depicts the relative location of Sabah with respect to the rest of Borneo and the relative location of the study area in Sabah.

The study area is comprised of a mixed landscape that includes areas of twice-logged forest (LF); virgin jungle reserve (VJR); oil palm (OP) plantations covering 45,016 ha and containing palm trees of varying age; 7200 ha of heavily logged area known as the experimental area (EA), which was earmarked for conversion to OP plantations beginning in December 2011; and undisturbed, OG, lowland primary forests in the Maliau Basin Conservation Area (MBCA). Figures 2(*b*) and (*c*) depict the layout of the MBCA, the location of the OG forests, and the layout of the mixed forests in the SAFE area (which in turn is located in the Yayasan Sabah Forest Concession area).

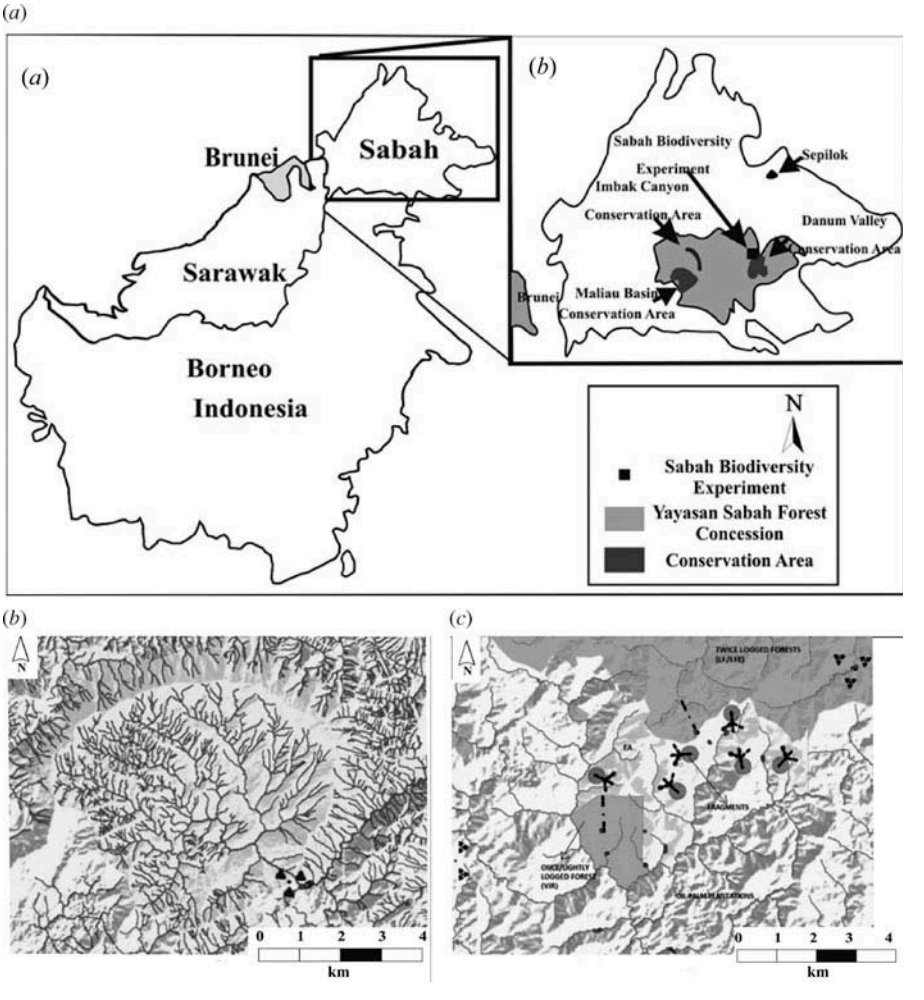

Figure 2. (*a*) Location of the study area in Sabah, Malaysia. (*b*) OG forests in Maliau Basin: lat 4.75, long 116.95. (*c*) Mixed forests: lat 4.75, long 117.6.

The EA is located in the Benta Wawasan area, which was last logged in the late 1990s. Logging was carried out intensively, including trees with diameter at breast height (DBH) of 30 cm, and effectively the entire pole was removed. The LF/LFE areas are located in the Ulu Segama river catchment, which has been selectively logged since the 1950s (Sabah Forestry Department, 2008 from Ancrenaz et al. (2010)). In the proposed OP concession, 800 ha of forest will be spared clearance and will be maintained in an arrangement of circular fragments together with a few riparian vegetation zones. The proposed circular fragments (A–F) have varying levels of forest cover. In addition to the riparian zones present in the EA, a number of riparian margins are present in the other land use types, including the OP plantations.

This study made use of the 193 vegetation plots designated previously as part of the SAFE project. These plots, which were established using the RAINFOR protocols (see RAINFOR 2012 for more details), measure 25 m × 25 m and are distributed across all different land-use types including primary forest, various stages of degradation and logging, and OP plantations (SAFE 2011). One of the main objectives of the establishment of these plots is to quantify the changes in carbon stocks after forest clearance and fragmentation, and thus, these plots were established across a land-use intensity gradient from slightly logged and LF stands of heavily degraded forests and OP plantations. Additionally, some vegetation monitoring plots were located in the unlogged primary forests in MBCA. Trees having a DBH greater than 10 cm were measured and tagged (Turner et al. 2012). In this study, we also surveyed the trees with DBH of 2–10 cm in subset plots. Based on these measurements, a small tree correction was calculated for each forest degradation type and then applied to the remaining plots. Calculations were performed using a dry matter approach.

An additional focus of this research was riparian forest plots. A riparian zone is defined as the land adjacent to streams and rivers. Malaysia contains 189 river systems, including 78 in Sabah. These zones enjoy legal protection and are maintained across all permanent water courses, although the width of these buffer zones varies according to state laws (Azliza et al. 2012). We established 90 riparian plots measuring 10 m × 50 m in the riparian zones of each of the different land-use types. For the purpose of creating a carbon inventory and collection of forest mensuration data, stratified random sampling is known to yield more precise estimates (MacDicken 1997). Selection of riparian zones and locations of the riparian plots was performed randomly to capture variation in spatial structure and biomass across the riparian zones. Three spatially distributed riparian zones were selected per land-use type. In each of the riparian zones, an additional six plots were set up 3–5 m from the river, with the 50 m side running parallel to the river. Thus, a total of 18 plots were created for each land-use type. Distances between the plots were not constant but were based on stratified random sampling, with the river serving as the baseline.

From these plots, forest mensuration data, namely DBH and height, were recorded using the RAINFOR protocols for all trees with DBH of 2 cm or more. The AGB (Mg ha $^{-1}$) of the trees in the riparian and non-riparian zones was calculated using the wet tropical forest biomass equation recommended by Chave et al. (2005), which is based on datasets from the tropical forests of Asia, Africa, and South America:

$$\text{Aboveground Biomass(AGB)} = 0.0776 \times \left(\rho \times \text{DBH}^2 \times H\right)^{0.94}. \quad (1)$$

In this equation, H refers to tree height and 0.0776 refers to wood specific gravity. Where the species were identified and data were available, species-specific values of ρ were

taken from Reyes et al. (1992); where the species were not known, a mean value for ρ of 0.57 g cm^{-3} from Brown (1997) was applied. This equation has been used previously to calculate AGB in Southeast Asian forests (Morel et al. 2011). Given the difference in the physiology of OP trees and trees in the forest, specific biomass equations were required in order to calculate the AGB of OP plantations. The AGB of OP trees was calculated using the biomass equation recommended by Morel, Fisher, and Malhi (2012):

$$(\mathrm{AGB})_{\mathrm{Trunk}} = 100 \times \Pi \times (r \times z)^2 \times h \times \rho', \tag{2}$$

where r is the radius of the trunk (cm) without frond bases, z is the ratio of the trunk diameter below the frond bases to the measured diameter above the frond bases (estimated to be 0.776 from the sampled trunks), and h is the height of the trunk (in m) to the base of the fronds. For this equation, ρ', the trunk density (in kg m^{-3}), was determined as follows:

$$\rho' = 0.0076x + 83/100, \tag{3}$$

where x is the age of the oil palm plantation. Both the SAFE vegetation plots and riparian plots are distributed across the SAFE study area, and field AGB values were calculated for all plots (see Figure 2(*c*)). In order to avoid the problems of auto-correlation and collinearity, randomly stratified samples were selected from the plots included in the study area. For each land-use type, 70% of the plots were selected randomly and used for calibration, and the remaining plots were used for validation.

2.2. *Remote-sensing data*

The SPOT-5 image includes five bands, including one panchromatic band with 5 m spatial resolution; two visible (green and red) bands with wavelengths of 0.5–0.59 μm and 0.61–0.68 μm, respectively; one near infrared (NIR) band with 10 m spatial resolution with wavelengths of 0.78–0.89 μm; and one short-wave infrared (SWIR) band with 20 m spatial resolution (Lu, Batistella, and Moran 2008) with wavelengths of 1.58–1.75 μm. The 20 m SWIR band is usually resampled to produce a 10 m image. The specific data acquisition process also allows an image sampled at 2.5 m to be produced from two 5 m resolution panchromatic images taken simultaneously. The combination of this 2.5 m image with a third, 10 m resolution image in multispectral mode results in a fused image composed of three bands (green, red, and NIR) to enhance the spatial resolution of the SPOT dataset. The 2.5 m SPOT images are thus a three-band colour image with a panchromatic view. Data fusion (without pan sharpening) of panchromatic bands with optical bands was performed to yield multi-band SPOT data with a spatial resolution of 2.5 m (Jones and Vaughan 2010). This spatial resolution is sufficient, albeit slightly more coarse than that in a previous study (Proisy, Couteron, and Fromard 2007). Atmospheric correction of the satellite data was carried out as a way of compensating for the atmospheric effects of scattering and absorption. This has to be undertaken before classification and change detection analysis of the images can be carried out. In this study, the dark object subtraction (DOS) method of atmospheric correction was performed. This is an image-based absolute atmospheric correction approach and is preferred for change detection and classification approaches (Foody, Boyd, and Cutler 2003).

2.3. Fourier-based textural ordination (FOTO)

2.3.1. Background

FOTO belongs to the family of spectral approaches that characterize digital images (such as those obtained from satellite data) along coarseness–fineness texture gradients (Barbier, Gastellu-Etchegorry, and Proisy 2010). FOTO makes use of multivariate ordination of Fourier spectra to classify canopy images with respect to canopy grain. The latter is a combination of mean size and frequency of tree crowns per sampling window (Ploton et al. 2012). The FOTO method has been used to distinguish between pristine forests and forests subjected to varying logging intensities. This method is also useful to predict biomass from forest canopy parameters obtained from remote-sensing data (Couteron, Barbier, and Gautier 2006; Ploton et al. 2012). The basic premise of the FOTO method is that frequency signatures relate well to components of the canopy grain size.

FOTO employs a combination of two techniques: 2D FFT is used to convert spatial information into the frequency domain, and ordination is performed by PCA (Proisy, Couteron, and Fromard 2007). Fourier transforms are important in the analysis of the repetitive structure of the canopy to break the intensity signal into sinusoidal waves of different spatial frequencies. This method has been used to analyse specific vegetation data from a wide range of frequencies obtained from VHR satellite data (Barbier, Gastellu-Etchegorry, and Proisy 2010).

SPOT data can be viewed using this ordination method to analyse spatial frequencies within the images in order to quantify the biomass patterns and intensities and to make predictions based on this information (Barbier et al. 2010; Couteron, Barbier, and Gautier 2006). This is an efficient method for analysing specific patterns found in the forest amongst the existing biomass, including canopies and related textual vegetation (Ploton et al. 2012).

2.3.2. Obtaining radial spectra from a 2D Fourier transform

The 2D Fourier analysis first removes any aspects of the images that are not critical to the analysis by converting data from the spatial domain to the frequency domain. The isolated irrelevant features include images related to shadows, water features, and man-made structures, which are not tied to biomass data. Then, the specific areas, in this case the different land-use types, are delineated from the whole image. These images are input into window-sized segments, in which the 2D Fourier spectra are computed. The window size (WS) is expressed in metres as $WS = N.\Delta S$, where N is the number of pixels in the X or Y direction and ΔS is the pixel size in metres (Proisy et al. 2012). The output of FOTO and subsequent biomass maps are directly influenced by WS; a higher WS may lead to the generation of coarser biomass maps by a factor of N (Proisy et al. 2012). After windowing the forest images, the individual windows are subjected to a 2D Fourier transformation.

Two-dimensional FFT is applied to sub-samples of VHR to obtain the radial spectra (or r-spectra) of the different forest types. Fourier r-spectra are computed for each window image from the remote-sensing data, determining the amplitude of each spatial frequency. A two-dimensional Fourier transformation allows for the decomposition of the total image variance according to all possible integer pairs (p, q) of wave numbers along the two Cartesian geographical directions. When expressed in polar form (Mugglestone and Renshaw 1998), these values are portions of image variance that is accounted for by a waveform having a spatial frequency r. These r-spectra are obtained through partitioning of image variance to different spatial frequency bins. R-spectra describe information about

the level of spatial variation in each spatial frequency (Proisy, Couteron, and Fromard 2007). The amplitude of the Fourier transform is squared to obtain the power spectrum, and the frequency is averaged in all azimuthal directions to produce the r-spectrum. The variation among the sampled frequencies can be linked with the structure and texture of the top canopy (Proisy, Couteron, and Fromard 2007). These values allow for the quantification of coarseness-related textural properties via study of the decomposition of variance among spatial frequencies. Images with a coarse texture will yield an r-spectrum that is skewed towards small wave numbers, whilst fine-textured images are expected to produce more balanced spectra (Couteron et al. 2005).

In this study, the window images of individual land use types were subjected to FFT using ENVI image processing software to obtain the power spectrum. The r-spectra were plotted with respect to the frequencies, which are expressed in cycles km^{-1} (Barbier et al. 2012). Figure 3 illustrates the steps in obtaining the r-spectra of the different land use types.

2.3.3. *Textural ordination of the radial-spectra*

A systematic textural analysis is carried out on the power spectrum of the individual land-use type images. The r-spectra are stacked into a common matrix in which each row corresponds to the r-spectrum of a given window. Each column contains amplitude values. These windows may be considered to be statistical observations characterized by their spectral profiles and may be subjected to ordination techniques, such as PCA (Proisy, Couteron, and Fromard 2007; Couteron, Barbier, and Gautier 2006; Barbier et al. 2010; Liu and Mason 2009; Ploton et al. 2012).

Spatial frequencies may be considered quantitative variables that are linearly combined to yield principal components (Couteron et al. 2005). Each principal component (PC) image represents a linear weighted combination of the original bands:

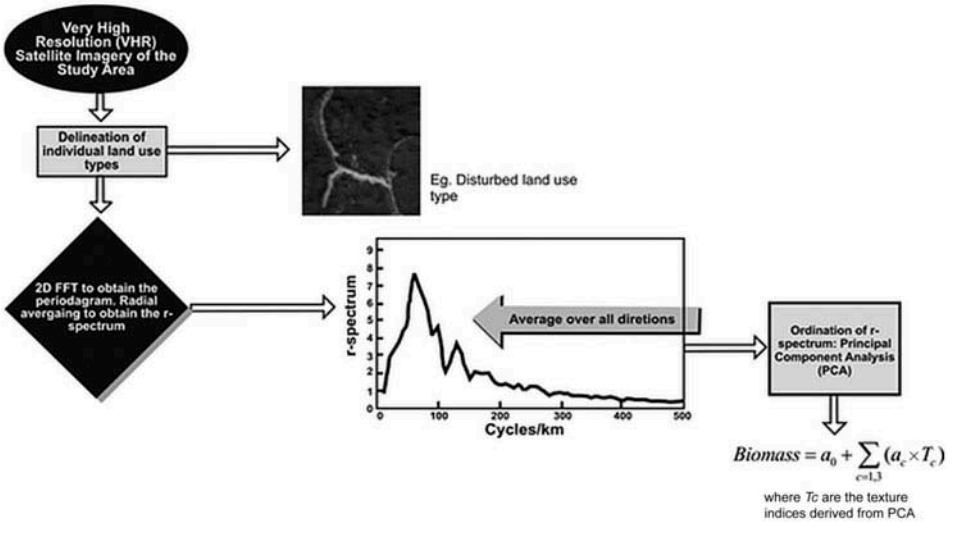

Figure 3. Obtaining radial spectra of individual land-use classes using the FOTO method (Adapted from Barbier, Gastellu-Etchegorry, and Proisy (2010).

$$PC_i = \sum_{k=1}^{m} g_{ik} \text{Band}_k. \quad (4)$$

The first principal component concentrates the features common to all original image bands. The images are square or rectangular extracts of relevant size, which is typically about 1 ha, or an area that is increasingly used for field plots to measure AGB in the tropics. PCA axes ordinate images along coarseness–finer gradients, sometimes also pointing out the dominant periodicity, if any, that mostly agrees with the visual appraisal (Couteron et al. 2005). The principal component variances decline sharply with increases in PC rank. In the case of satellite-based vegetation analysis, bands up to PC3 highlight the vegetation contrasts. Hence, only the first three PC axes are retained for further analysis (Liu and Mason 2009). The three most prominent components obtained from application of PCA are taken as the texture indices (Proisy et al. 2012). The texture indices obtained from the FOTO method can be subjected to multiple linear regressions to characterize the spatial structure and texture of vegetation, especially structural parameters that are connected to the upper canopy (Ploton et al. 2012). Via crown areas, FOTO results are further correlated with stand parameters such as basal area and diameter at breast height, rendering these data useful for evaluating the AGB of a given area (Barbier, Gastellu-Etchegorry, and Proisy 2010). The AGB data obtained from the plots located in the different land-use types were regressed against these texture indices to obtain biomass estimate models for the different land use types.

3. Results

In this study, multiple forest types, including OG, forests logged at varying intensities, and OP plantations, were sampled using remote-sensing data from both riparian and non-riparian zones. The basic parameters of the plots sampled are shown in Tables 1 and 2.

The FOTO method was applied to sub-samples of VHR SPOT imagery of the identified plots in Sabah, Malaysia in order to distinguish between the different types of forest, based on land-use parameters as well as to develop individual biomass estimates for each. Different land-use types yield different r-spectrum curves and peak frequencies, as shown in Figure 4.

Furthermore, the r-spectra captured the whole canopy grain gradient, ranging from pristine OG forests to logged forests to OP plantations. Across the different forest types, the dominant frequencies varied from 57 cycles km^{-1} (λ = 17.5 m) for OP to 82 cycles km^{-1} (λ = 12.2 m) for riparian forests, and 135 cycles km^{-1} (λ = 7.4 m) for OG forests to 180 cycles km^{-1} (λ = 5.55 m) for once/lightly logged forests. This finding suggests that disturbance increased the dominant spatial dimensions of the canopy texture in the sampled forests.

Column-wise standardization was performed on r-spectra data. Standardized PCA was performed on the unit window. PCA ordination allows for the interpretation of the cloud of unit windows in terms of canopy grain variation, ranging from fine to coarse scale. The results of the PCA yielded three prominent axes, which synthesized the majority of the variability in the data matrix. The first principle component (PC1) explains the largest percentage (48%) of the variance and appears to capture the fineness–coarseness gradient of the canopy grain, as depicted in Figure 5. Furthermore, PC2 has the highest value of riparian forests and the lowest (negative) values for OG forests and OP plantations, which both have contiguous canopies.

Table 1. Above-ground forest parameters across the riparian (RF) margins.

	$(OG)_{RF}$	$(VJR)_{RF}$	$(LF)_{RF}$	$(EA)_{RF}$	$(OP)_{RF}$
Basal area (m^2 ha^{-1})	56.28 ± 9.27	55 ± 8.1537	49.75 ± 9.19	29.146 ± 5.52	34.183 ± 3.205
Basal area of trees with DBH >10 cm (m^2 ha^{-1})	55.8 ± 8.878	54.486 ± 7.98	48 ± 9.74	25.289 ± 5.18	32.44 ± 3.18
Tree height (m)	19.7 ± 0.83	18.9 ± 1.31	22.7 ± 1.44	9.2 ± 0.33	9.7 ± 0.25
Stem density (ha^{-1})	667	714	629	840	1056
Stem density of trees with DBH >10 cm (ha^{-1})	488	481	456	440	601

Note: For these data, n = 18 riparian plots for each of the land-use types. OG, old-growth forests; VJR, virgin jungle reserve; LF, logged forest; EA, experimental area; OP, oil palm plantations.

Table 2. Above-ground forest parameters across the non-riparian zones (NRF).

	$(OG)_{NRF}$	$(LF)_{NRF}$	$(EA)_{NRF}$
Basal area of trees with DBH >10 cm (m^2 ha^{-1})	65.39 ± 3.1	32.13 ± 13.43	17.14 ± 2.17
Stem density of trees with DBH >10 cm (ha^{-1})	820	592	417

Note: OG, old-growth forests; LF, logged forest; EA, experimental area.

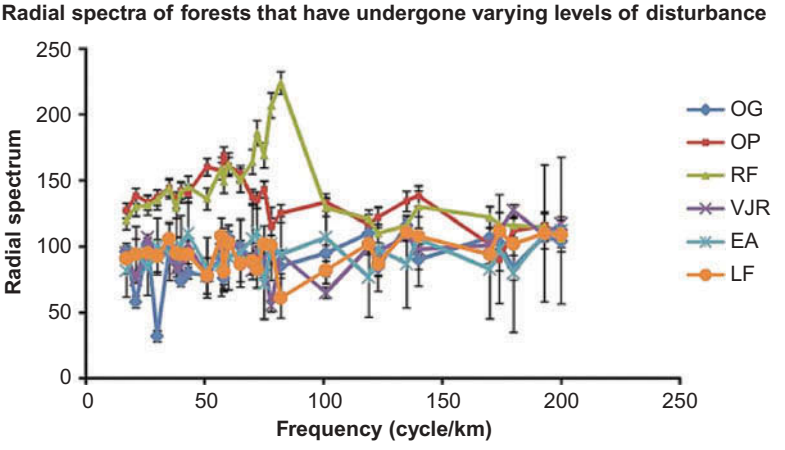

Figure 4. Radial spectra of individual land-use classes with respect to frequency (cycles km^{-1}). OG, old-growth forests; OP, oil palm plantations; RF, riparian forests; VJR, virgin jungle reserve; EA, experimental area; LF, twice-logged forests.

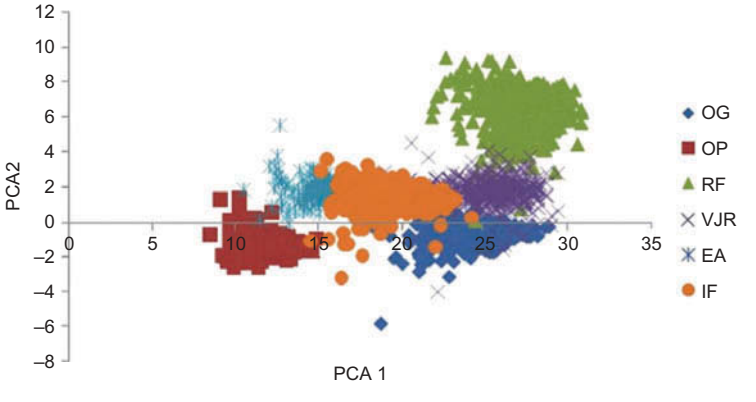

Figure 5. PCA on FOTO-derived r-spectra. Top: PCA1 vs. PCA2 location of r-spectra of the different land-use types. Bottom: histogram of Eigenvalues showing the percentage of variance explained by each PCA axis in sequence (OG, old-growth forests; OP, oil palm plantations; RF, riparian forests; VJR, virgin jungle reserve; EA, experimental area; LF, twice-logged forests).

The first three principal axes were taken to be the texture indices, which, in turn, can be used to correlate the stand parameters and biomass dynamics of the different land-use types. According to the research of Couteron et al. (2005), PC1 also acts as a sound predictive variable to explain the variations in stand structure. Data in our study confirmed

this finding. For instance, PC1 explained approximately 30% of the variation in DBH of OG forest trees and 36.6% variation in the basal area of OG forests. PC1 also explained 28% of the variation in DBH of heavily logged forests and 16% of the variation in the basal area of this land-use type.

The texture indices were derived in order to generate biomass estimate models for the different land-use types in the study area. All three FOTO-derived texture indices were related to field AGB values of the 70% of the plots per land-use type that were randomly selected (discussed in Section 2.1) using multiple regressions. These analyses were performed in order to derive biomass estimate models for individual land-use types. The FOTO-derived biomass estimate equations for the individual land-use type are detailed in Table 3.

Stands may actually display similar AGB values despite contrasting stages of the disturbance and distinct canopy textures (Proisy et al. 2002). Hence, a Tukey test was performed to determine whether the canopy texture-based biomass estimate models significantly varied across different land-use types. The biomass estimate models varied significantly between the riparian forests, LF, once/slightly logged forests, and OP plantations. Unsurprisingly, the biomass values derived from the canopy texture-based biomass estimate model for OP plantations were significantly different from the other non-riparian land use texture-based biomass model values. Furthermore, the texture-based biomass values were significantly different from OG pristine forests, once/slightly logged, and heavily logged forests. A FOTO biomass map of the SAFE area was created in Figure 6 using the equations presented in Table 3. The SAFE study site has a significant proportion of forests that have undergone two or more rounds of logging. FOTO-derived biomass values indicated that LF have an AGB of 120–155 Mg ha^{-1}, while OP plantations have the lowest FOTO-derived AGB values, 0–80 Mg ha^{-1}; the lightly logged forests or the VJR showed very high values for FOTO-derived AGB (180–270 Mg ha^{-1}). Small patches of unlogged forest tracts have the highest FOTO-derived AGB values, ranging from 270 to 372 Mg ha^{-1}. These values are in agreement with field AGB values obtained previously in this region (Morel et al. 2011). A bar graph comparing the differences in FOTO AGB values of the main land use types is shown in Figure 7.

The FOTO-derived AGB values were validated against the field AGB values, which were determined from the remaining randomly stratified plots that were not used for calibration of all land-use types. In order to measure the goodness of fit, R^2 values were assessed for combined and individual land-use types as shown in Figure 8.

Table 3. SPOT texture indices-based biomass equations derived using field AGB values.

Land-use type	FOTO texture-based indices	R^2
Old-growth (OG) forest	−59.51 × (PC1) − 45.551 (PC2) − 4.936 × (PC3) + 1743.287	0.97
Once/lightly logged forest (VJR)	−493.51 × (PC1) + 2792.2g(PC2) + 2882(PC3) + 7653.62	0.905
Twice-logged forest (LF)	−83.44 × (PC1) + 1049.78g(PC2) − 32.13. (PC3) + 289.1	0.811
Heavily logged forest (EA)	20.71(PC1) + 280.82 (PC2) − 34.47 × (PC3) − 222.1	0.955
Riparian forest (RF)	−240.6 × (PC1) − 632.66a(PC2) + 180.47 × (PC3) + 3136.8	0.84
Oil palm plantation (OP)	−4773.26 × (PC1) + 5171(PC2) − 1817.546(PC3) + 61036.76	0.83

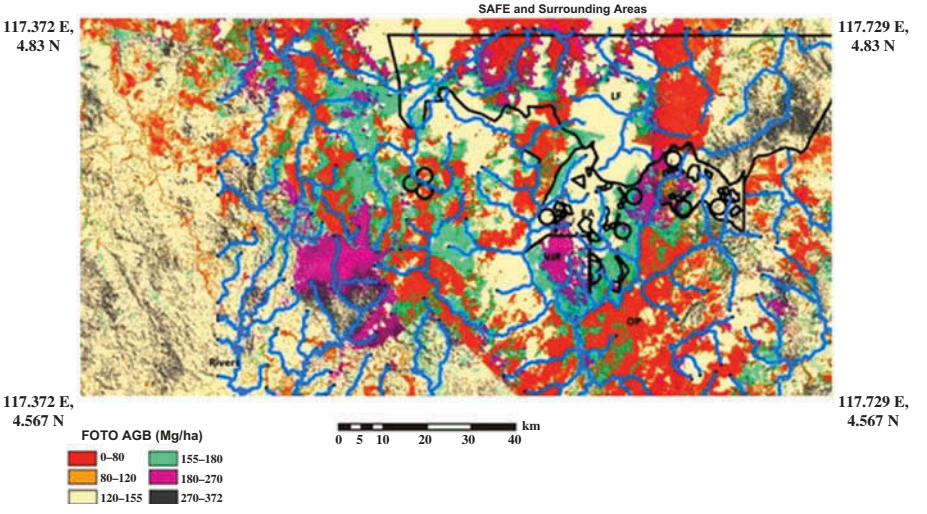

Figure 6. FOTO-generated biomass map of the SAFE area (VJR, virgin jungle reserve; LF, logged forest; EA, experimental area; OP, oil palm plantations). Blue lines represent the river network in the area.

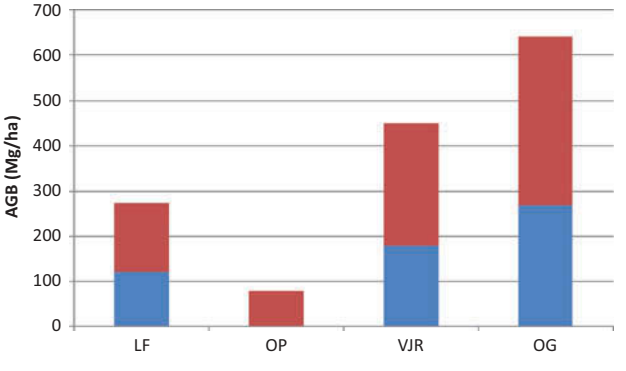

Figure 7. Bar graph comparing the differences in the FOTO AGB values of the main land-use types. The maroon bars depict the actual variation in FOTO AGB values for the different land-use types.

Initially, regression analysis was carried out for all land-use types, and the FOTO-derived and field AGB values were strongly correlated ($R^2 = 0.9795$, $p = 0.000352$). The difference between the slope of the actual and the expected regression lines was minimal, and thus the texture-derived indices predict AGB with great accuracy. The FOTO-derived AGB values showed no evidence of saturation at high biomass values.

FOTO-derived AGB values for individual land-use types were also validated against field AGB values. Specifically, validation was performed for three individual land-use types: old growth, VJR, and EA. Regression analysis of FOTO-derived AGB values against field AGB values yielded slopes that were indistinguishable from 1:1 and with low scatter (for OG, slope = 1.125 ± 0.0955, $R^2 = 0.853$, $p = 0.007$; EA, slope = 0.78 ± 0.051, $R^2 = 0.9564$, $p = 0.000131$; VJR, slope = 0.945 ± 0.067,

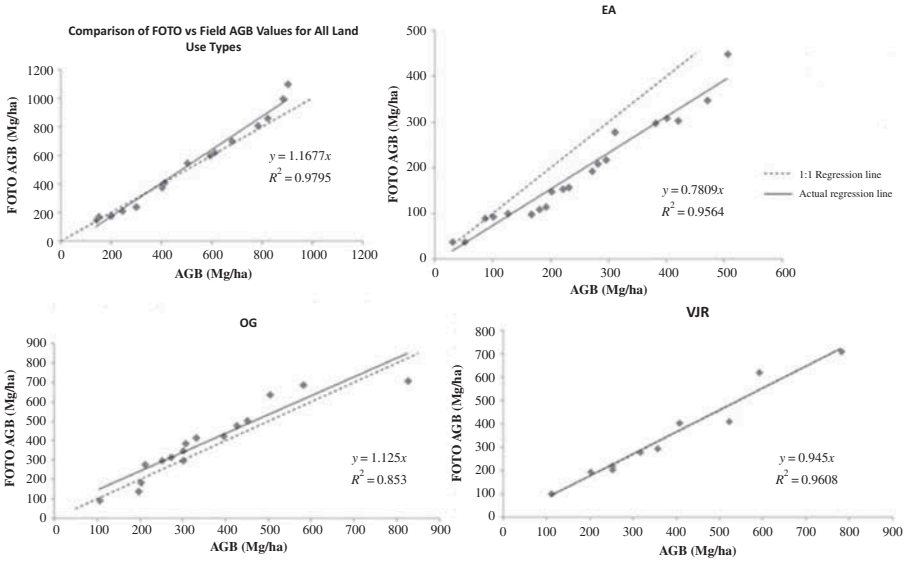

Figure 8. Regression analysis of FOTO-derived AGB values vs. field AGB values for: (*a*) all land-use types, (*b*) heavily logged forests, (*c*) old growth forests, and (*d*) lightly logged forests.

R^2 = 0.9608, p = 0.042). The OG and VJR forests also exhibited strong agreement with the expected regression line and showed little deviation in the slope of expected and actual regression lines; however, in the case of EA, the FOTO-derived texture indices underestimated the ground AGB values by approximately 22%.

4. Discussion

One of the major uncertainties in estimation of AGB in tropical forests, especially in the context of large-scale land-use change and forest degradation, is the use of allometric equations (Grainger 2010). A significant challenge is the presence of a complex canopy structure and saturation of non-textural remote-sensing approaches at high biomass values (Williams et al. 2011; Malhi and Roman-Cuesta 2008). Direct regressions with optical and radar data are affected by saturation (Mitchard et al. 2011); however, FOTO allows for the discrimination of structural and biomass variation in different land use types and avoids the issue of saturation at high biomass values.

The use of Fourier transforms and subsequent ordination using PCA is the basis of the FOTO method. The frequency signatures relate effectively to the components of the canopy grain size (Couteron, Barbier, and Gautier 2006). This methodology has been effective in representing and analysing the repetitive structure of the canopy. It has been inferred that r-spectra allow differentiation of the different forest structures in the study area. For example, riparian forests display a markedly distinct r-spectrum profile compared with other land-use types. Hence, riparian forests may be considered to be structurally different from surrounding, non-riparian land-use types. Similarly, other land-use types display varying r-spectra and peak frequencies, indicating that the different forest types have different canopy structures, which, in turn, are reflected in their frequency signals. The PCA ordination of the r-spectra of the different land-use types also allows for differentiation between the different forest types and facilitates the description of the

overall variation in the texture of the different forest types in the study area. This data, in turn, allows evaluation of the degree of fragmentation and disturbance faced by the individual forest types. For instance, the PCA1 vs. PCA2 plot indicates that riparian forest is the least homogenous of forest types and has faced very high levels of fragmentation. This has been verified from ground surveys. In our analysis, PCA1 explained the largest portion (48%) of the variance and appeared to capture the fineness–coarseness gradient of the canopy grain, as observed in Figure 5. This, in turn, is linked to the dominant crown size (Barbier et al. 2012) and corresponds to spatial frequencies of less than 80 cycles km^{-1} (wavelength = 12.5 m) for coarser textures to more than 180 cycles km^{-1} (wavelength = 5.56 m) for finer textures (Proisy, Couteron, and Fromard 2007). Other PCA axes may point to a specific range of dominant spatial frequencies, which may be related to crown or gap sizes (Barbier et al. 2012). Hence, PCA1 represents the disturbance gradient faced by the different land-use types. On the other hand, the results suggest that PCA2 explains the degree of fragmentation faced by the different land-use types. Relatively homogenous/undisturbed forest types such as OG and OP have lower values for PCA2. Field studies revealed that riparian forests exist as fragmented patches throughout the landscape and, as such, PCA2 has the highest value for riparian forests and lowest (negative) values for OG and OP plantations, which have contiguous canopies as depicted in Figure 5.

Similarly, the results of PCA have been useful in allowing for the examination of the disturbance–fragmentation gradient of other land-use types. For instance, OG forests and OP plantations, both of which have a fairly contiguous canopy structure, stretched along the PCA1 axis. On average, for all the land-use types combined, the FOTO-derived estimate models predicted the biomass well. The variation in the ability of FOTO to predict biomass values across different land-use types may be related to the degree of disturbance and fragmentation. For instance, the EA (for which the FOTO approach underestimates the AGB) has a high degree of disturbance, and such high heterogeneity may lead to the calibration dataset being insufficient to capture the degrees of heterogeneity within this forest type. On the other hand, both OG and VJR forests have experienced relatively small disturbance and fragmentation, and the FOTO method appears to estimate biomass well and consistently. Hence, these findings suggest that the predictive ability of the FOTO algorithm may be influenced by the degree of disturbance and fragmentation dynamics of a given forest type.

Overall, this method has proved effective in distinguishing between OP plantations and the surrounding tropical forest. More importantly, this technique allowed differentiation between forests that have undergone varying logging practices. In addition, this technique allowed for identification of forests (in this case, riparian forests) that have become isolated within a given land-use type. Therefore, these analyses indicate that this methodology is useful in distinguishing between the different levels of disturbance, such as logging and degradation, across the land-use types within the forest areas. This analysis achieved the first objective, which was to distinguish between different land-cover types, including forests of different logging intensities, OP plantations, and pristine forests using the FOTO method. Furthermore, this study illustrates that the FOTO method has significant potential as a system for predicting biomass changes among OP–tropical forest landscapes in order to track the impact of various logging cycles to better assess the current and future impact of such activity. As in other studies (Proisy, Couteron, and Fromard 2007; Ploton et al. 2012), the FOTO method was effective in predicting forest AGB. As such, this methodology not only provides accurate structural information about the uppermost portions of the forest canopies but also offers this same level of information

about sub-canopy characteristics and changes (Ploton et al. 2012), thus satisfying the second objective, which was to develop texture-based biomass estimate models for different land-use types. No specific procedures have been developed to provide spatial and structural information about the conditions of riparian margins (Johansen and Phinn 2006); however, use of the FOTO method in this study has allowed for assessment of the structure at riparian margins, in addition to ascertaining that these characteristics vary between riparian and non-riparian zones. These findings satisfied the third objective, which was to examine the possibility of distinguishing a remnant/isolated forest ecosystem, such as riparian forests, from surrounding contiguous forest types. The ability to discriminate the biomass and structure of riparian zones from non-riparian zones has significant implications for examining the impact of fragmentation and land-use change on the structural and biomass dynamics of remnant ecosystems, such as riparian forests. Forest fragmentation may lead to elevated tree mortality and micro-climatic changes at the edges, which, in turn, can lead to changes in structure, biomass stocks, and carbon fluxes in the forest fragments (Nascimento and Laurance 2004).

5. Conclusion

This study presented the use the Fourier Transform Ordination (FOTO) method to determine above-ground biomass and canopy structure of various Malaysian land-cover types. The generation of texture maps of these forest landscapes based on the analysis of high-resolution satellite data by the FOTO method, in conjunction with ground data collection and experiments such as those of the SAFE project, provided some valuable insight on the biomass of each forest. This information may provide the foundation for changing logging patterns and human activity in these valued forest landscapes, thereby reducing forest degradation and increasing ecological recovery. It is noted, however, that the FOTO-derived biomass estimate models are ultimately based on field AGB values. Inaccuracies and uncertainties perpetuated in the allometric equations may influence the texture-based AGB estimates. Furthermore, the predictive ability of the FOTO algorithm may be influenced by the degree of disturbance and fragmentation of a given forest type.

Compared with methods based on spectral characteristics, texture-based methods have the potential to sidestep the problems of saturation that result in the prediction of relatively higher biomass values. Texture-based methods, including FOTO, along with the use of satellite and field data, may also serve other purposes and offer help to more tropical forest countries and areas to more effectively monitor their forest cover and track the ongoing evolution and changes in the forest and related biomass.

Acknowledgements

The authors are grateful to the following individuals and institutions for their valuable help in making this research possible: Sime Darby, Dr Rob Ewers, Dr Ed Turner, Dr Glenn Reynolds, Sabah Biodiversity Centre (SABC), the Royal Society's South East Asia Rainforest Research Programme (SEARRP), and the Stability of Altered Forest Ecosystems (SAFE) project.

References

Ancrenaz, M., L. Ambu, I. Sunjoto, E. Ahmad, K. Manokaran, E. Meijaard, and I. Lackman. 2010. "Recent Surveys in the Forests of Ulu Segama Malua, Sabah, Malaysia, Show That Orang-utans (P. p. morio) Can Be Maintained in Slightly Logged Forests." *PLoS ONE* 5 (7): e11510. doi:10.1371/journal.pone.0011510.

Azliza, M., M. Nazre, M. K. Mohamad-Roslan, and K. Shamsul. 2012. "Characterization of Riparian Plant Community in Lowland Forest of Peninsular Malaysia." *International Journal of Botany* 8: 181–191.

Barbier, N., P. Couteron, J.-P. Gastelly-Etchegorry, and C. Proisy. 2012. "Linking Canopy Images to Forest Structural Parameters: Potential of a Modeling Framework." *Annals of Forest Science* 69 (2): 305–311. doi:10.1007/s13595-011-0116-9.

Barbier, N., P. Couteron, C. Proisy, Y. Malhi, and J.-P. Gastellu-Etchegorry. 2010. "The Variation of Apparent Crown Size and Canopy Heterogeneity Across Lowland Amazonian Forests." *Global Ecology and Biogeography* 19 (1): 72–84. doi:10.1111/j.1466-8238.2009.00493.x.

Barbier, N., J.-P. Gastellu-Etchegorry, and C. Proisy. 2010. "Assessing Forest Structure and Biomass from Canopy Aspect Analysis on Metric Resolution Remotely-sensed Images." CarboAfrica Conference, Pointe Noire, March 17–19.

Barker, M., and M. Pinard. 2001. "Forest Canopy Research: Sampling Problems, and Some Solutions." *Plant Ecology* 153 (1/2): 23–38. doi:10.1023/A:1017584130692.

Basuki, T., A. Skidmore, P. van Laake, I. van Duren, and Y. Hussin. 2012. "The Potential of Spectral Mixture Analysis to Improve the Estimation Accuracy of Tropical Forest Biomass." *Geocarto International: A Multidisciplinary Journal of Remote Sensing* 27 (4): 329–345. doi:10.1080/10106049.2011.634928.

Brioch, M., M. Hansen, F. Stolle, P. Potapov, M. Arunarwati, and B. Adusei. 2011. "Remotely Sensed Forest Cover Loss Shows High Spatial and Temporal Variation Across Sumatera and Kalimantan, Indonesia 2000–2008." *Environmental Research Letters* 6 (1): 277–291.

Brown, S. 1997. *Estimating Biomass and Biomass Change for of Tropical Forests: A primer*. Rome: FAO.

Chambers, J. Q., G. P. Asner, D. C. Morton, L. O. Anderson, S. S. Saatchi, F. D. B. Espírito-Santo, M. Palace, and C. Souza. 2007. "Regional Ecosystem Structure and Function: Ecological Insights from Remote Sensing of Tropical Forests." *Trends in Ecology & Evolution* 22 (8): 414–423. doi:10.1016/j.tree.2007.05.001.

Chave, J., C. Andalo, S. Brown, M. A. Cairns, J. Q. Chambers, D. Eamus, H. Fölster, F. Fromard, N. Higuchi, T. Kira, J.-P. Lescure, B. W. Nelson, H. Ogawa, H. Puig, B. Riéra, and T. Yamakura. 2005. "Tree Allometry and Improved Estimation of Carbon Stocks and Balance in Tropical Forests." *Oecologia* 145 (1): 87–99. doi:10.1007/s00442-005-0100-x.

Couteron, P., N. Barbier, and D. Gautier. 2006. "Textural Ordination Based on Fourier Spectral Decomposition: A Method to Analyze and Compare Landscape Patterns." *Landscape Ecology* 21 (4): 555–567. doi:10.1007/s10980-005-2166-6.

Couteron, P., R. Pelissier, E. Nicolini, and D. Paget. 2005. "Predicting Tropical Forest Stand Structure Parameters from Fourier Transform of Very High-Resolution Remotely Sensed Canopy Images." *Journal of Applied Ecology* 42: 1121–1128.

Eckert, S. 2012. "Improved Forest Biomass and Carbon Estimations Using Texture Measures from WorldView-2 Satellite Data." *Remote sensing* 4 (4): 810–829. doi:10.3390/rs4040810.

Ewers, R., R. Didham, L. Fahrig, Ferraz G., Hector A., Holt R. D., Kapos V., Reynolds G., Sinun W., Snaddon J. L., and Turner E. C. 2011. "A Large-Scale Forest Fragmentation Experiment: The Stability of Altered Forest Ecosystems Project." *Philosophical Transactions of the Royal Society B Biological Sciences* 366 (1582): 3292–3302. doi:10.1098/rstb.2011.0049.

Foody, G. M., D. S. Boyd, and M. E. J. Cutler. 2003. "Predictive Relations of Tropical Forest Biomass from Landsat TM Data and Their Transferability between Regions." *Remote Sensing of Environment* 85 (4): 463–474.

Gibbs, H. K., S. Brown, J. O. Niles, and J. A. Foley. 2007. "Monitoring and Estimating Tropical Forest Carbon Stocks: Making REDD a Reality." *Environmental Research Letters* 2 (4): 045023. doi:10.1088/1748-9326/2/4/045023.

Grainger, A. 2010. "Uncertainty in the Construction of Global Knowledge of Tropical Forests." *Progress in Physical Geography* 34 (6): 811–844. 10.1177/0309133310387326.

Hawes, J. E., C. A. Peres, L. B. Riley, and L. L. Hess. 2012. "Landscape-Scale Variation in Structure and Biomass of Amazonian Seasonally Flooded and Unflooded Forests." *Forest Ecology and Management* 281: 163–176. doi:10.1016/j.foreco.2012.06.023.

Helmer, E. H., T. S. Ruzycki, J. Benner, S. M. Voggesser, B. P. Scobie, C. Park, D. W. Fanning, and S. Ramnarine. 2012. "Detailed Maps of Tropical Forest Types are Within Reach: Forest Tree Communities for Trinidad and Tobago Mapped with Multiseason Landsat and Multiseason

Fine-Resolution Imagery." *Forest Ecology and Management* 279: 147–166. doi:10.1016/j.foreco.2012.05.016.

Huete, A., K. Didan, T. Miura, E. P. Rodriguez, X. Gao, and L. G. Ferreira. 2002. "Overview of the Radiometric and Biophysical Performance of the MODIS Vegetation Indices." *Remote Sensing of Environment* 83 (1–2): 195–213. doi:10.1016/S0034-4257(02)00096-2.

Ingram, J. C., T. P. Dawson, and R. J. Whittaker. 2005. "Mapping Tropical Forest Structure in Southeastern Madagascar using Remote Sensing and Artificial Neural Networks." *Remote Sensing of Environment* 94 (4): 491–507. doi:10.1016/j.rse.2004.12.001.

Johansen, K., and S. Phinn. 2006. "Mapping Structural Parameters and Species Composition of Riparian Vegetation Using IKONOS and Landsat ETM+ Data in Australian Tropical Savannahs." *Photogrammetric Engineering & Remote Sensing* 72 (1): 71–80. doi:10.14358/PERS.72.1.71.

Jones, H. G., and R. A. Vaughan. 2010. *Remote Sensing of Vegetation: Principles, Techniques, and Applications*. New York: Oxford University Press.

Jong, S. M., and F. Van der Meer. 2004. *Remote Sensing Image Analysis: Including the Spatial Domain*. Utrecht: Springer.

Liu, J. G., and P. Mason. 2009. *Essential Image Processing and GIS for Remote Sensing*. New York: Wiley.

Lu, D. 2006. "The Potential and Challenge of Remote Sensing-Based Biomass Estimation." *International Journal of Remote Sensing* 27: 1297–1328. doi:10.1080/01431160500486732.

Lu, D., M. Batistella, and E. Moran. 2008. "Integration of Landsat TM and SPOT HRG Images for Vegetation Change Detection in the Brazilian Amazon." *Photogrammetric Engineering and Remote Sensing* 74 (4): 421–430.

Lu, D., M. Batistella, E. Moran, and P. Mausel. 2004. "Application of Spectral Mixture Analysis to Amazonian Land-Use and Land-Cover Classification." *International Journal of Remote Sensing* 25 (23): 5345–5358. doi:10.1080/01431160412331269733.

Lu, D., Q. Chen, G. Wang, E. Moran, M. Batistella, M. Zhang, G. V. Laurin, and D. Saah. 2012. "Above-ground Forest Biomass Estimation with Landsat and LiDAR Data and Uncertainty Analysis of the Estimates." *International Journal of Forestry Research* doi:10.1155/2012/436537.

MacDicken, K. 1997. *A Guide to Monitoring Carbon Storage in Forestry and Agroforestry Projects*. Little Rock, AR: Winrock International Institute for Agricultural Development.

Malhi, Y., L. E. O. C. Aragao, D. Galbraith, C. Huntingford, R. Fisher, P. Zelazowski, S. Sitch, C. McSweeney, and P. Meir. 2009. "Exploring the Likelihood and Mechanism of a Climate-Change-Induced Dieback of the Amazon Rainforest." *Proceedings of the National Academy of Sciences* 106 (49): 20610–20615. doi:10.1073/pnas.0804619106.

Malhi, Y., and R. M. Román-Cuesta. 2008. "Analysis of Lacunarity and Scales of Spatial Homogeneity in IKONOS Images of Amazonian Tropical Forest Canopies." *Remote Sensing of Environment* 112 (5): 2074–2087. doi:10.1016/j.rse.2008.01.009.

Mitchard, E. T. A., S. S. Saatchi, L. J. T. White, K. A. Abernethy, K. J. Jeffery, S. L. Lewis, M. Collins, M. A. Lefsky, M. E. Leal, I. H. Woodhouse, and P. Meir. 2011. "Mapping Tropical Forest Biomass with Radar and Spaceborne LiDAR in Lopé National Park, Gabon: Overcoming Problems of High Biomass and Persistent Cloud." *Biogeosciences* 9: 179–191. doi:10.5194/bg-9-179-2012.

Morel, A. C. 2010. "Environmental Monitoring of Oil Palm Expansion in Malaysian Borneo and Analysis of Two International Governance Initiatives Relating to Palm Oil Production." DPhil Thesis, University of Oxford.

Morel, A. C., J. B. Fisher, and Y. Malhi. 2012. "Evaluating the Potential to Monitor Aboveground Biomass in Forest and Oil Palm in Sabah, Malaysia, for 2000–2008 with Landsat ETM+ and ALOS-PALSAR." *International Journal of Remote Sensing* 33: 3614–3639.

Morel, A. C., S. S. Saatchi, Y. Malhi, N. J. Berry, L. Banin, D. Burslem, R. Nilus, and R. C. Ong. 2011. "Estimating Above-ground Biomass in Forest and Oil Palm Plantation in Sabah, Malaysian Borneo using ALOS PALSAR Data." *Forest Ecology and Management* 262 (9): 1786–1798. doi:10.1016/j.foreco.2011.07.008.

Mugglestone, M. A., and E. Renshaw. 1998. "Detection of Geological Lineations on Aerial Photographs using Two Dimensional Spectral Analysis." *Computers & Geosciences* 24 (8): 771–784. doi:10.1016/S0098-3004(98)00065-X.

Nascimento, H., and W. F. Laurance. 2004. "Biomass Dynamics in Amazonian Forest Fragments." *Ecological Applications* 14 (sp4): S127–S138. doi:10.1890/01-6003.

Nichol, J. E., and M. L. R. Sarker. 2011. "Improved Biomass Estimation using the Texture Parameters of Two High Resolution Optical Sensors." *IEEE Transactions on Geoscience and Remote Sensing* 49 (3): 930–948. doi:10.1109/TGRS.2010.2068574.

Pearson, T., S. Brown, S. Petrova, N. Moore, and D. Slaymaker. 2005. *Application of Multispectral Three-dimensional Aerial Digital Imagery for Estimating Carbon Stocks in a Closed Tropical Forest (Report to the Nature Conservancy Conservation Partnership Agreement)*. Arlington, VA: Winrock International. http://www.winrock.org/ecosystems/files/WI_Belize_ClosedForest_M3DADI_Report_2005.pdf

Ploton, P., R. Pélissier, C. Proisy, T. Flavenot, N. Barbier, S. N. Rai, and P. Couteron. 2012. "Assessing Above Ground Tropical Forest Biomass using Google Earth Canopy Images." *Ecological Applications* 22 (3): 993–1003. doi:10.1890/11-1606.1.

Proisy, C., N. Barbier, M. Guéroult, R. Pélissier, J.-P. Gastellu-Etchegorry, E. Grau, and P. Couteron. 2012. Biomass Prediction in Tropical Forests: The Canopy Grain Approach. In *Remote Sensing of Biomass – Principles and Applications*, edited by T. Fatoyinbo, InTech. http://cdn.intechopen.com/pdfs/33851/InTech-Biomass_prediction_in_tropical_forests_the_canopy_grain_approach.pdf

Proisy, C., P. Couteron, and F. Fromard. 2007. "Predicting and Mapping Mangrove Biomass from Canopy Grain Analysis using Fourier-Based Textural Ordination of IKONOS Images." *Remote Sensing of Environment* 109 (3): 379–392. doi:10.1016/j.rse.2007.01.009.

Proisy, C., E. Mougin, F. Fromard, V. Trichon, and M. A. Karam. 2002. "On the Influence of Canopy Structure on the Radar Backscattering of Mangrove Forests." *International Journal of Remote Sensing* 23 (20): 4197–4210. doi:10.1080/01431160110107725.

RAINFOR. 2012. *Amazon Forest Inventory Network*. http://www.geog.leeds.ac.uk/projects/rainfor/

Reyes, G., S. Brown, J. Chapman, and A. E. Lugo. 1992. "Wood Densities of Tropical Tree Species." United States Department of Agriculture, 98 Forest Service Southern Forest Experimental Station, New Orleans. General Technical Report SO–88.

Stability of Altered Forest Ecosystems (SAFE). 2011. http://www.safeproject.net/

Souza, C. M., D. A. Roberts, and A. Monteiro. 2005. "Multi-Temporal Analysis of Degraded Forests in the Southern Brazilian Amazon." *Earth Interactions* 9 (19): 1–25. doi:10.1175/EI132.1.

Turner, E. C., Y. Z. Abidin, H. Barlow, T. M. Fayle, M. H. H. Jaafar, C. V. Khen, J. Larenus, A. Nainar, G. Reynolds, Y. B. Yusof, M. S. Khoo, and R. M. Ewers. 2012. "The Stability of Altered Forest Ecosystems Project: Investigating the Design of Human-Modified Landscapes for Productivity and Conservation." *The Planter* 88: 453–468.

Wijaya, A., S. Kusnadi, R. Gloaguen, and H. Heilmeier. 2010. "Improved Strategy for Estimating Stem Volume and Forest Biomass using Moderate Resolution Remote Sensing Data and GIS." *Journal of Forestry Research* 21 (1): 1–12. doi:10.1007/s11676-010-0001-7.

Williams, M. L., S. Silman, S. Saatci, S. Hensley, M. Sanford, A. Yohannan, B. Kofman, J. Reis, and B. Kampes. 2011. "Analysis of GeoSAR Dual-band InSAR Data for Peruvian Forest." International Geoscience and Remote Sensing Symposium (IGARSS) 2010, Article Number 5651188, 1398–1401. Honolulu, HI: IEEE.

Woodhouse, I. H., E. T. A. Mitchard, M. Brolly, D. Maniatis, and C. M. Ryan. 2012. "Radar Backscatter is Not a 'Direct Measure' of Forest Biomass." *Nature Climate Change* 2: 556–557. doi:10.1038/nclimate1601.